Quantum Chemical Study of the Inhibitive Properties of 2-Pyridyl-Azoles

Badhin Gómez,*,† N. V. Likhanova,† M. A. Domínguez-Aguilar,† R. Martínez-Palou,† Alberto Vela,‡ and José L. Gázquez*,§

Programa de Ingeniería Molecular, Competencia de Química Aplicada, Instituto Mexicano del Petróleo, Eje Central Lázaro Cárdenas No. 152, San Bartolo Atepehuacan, México, D. F., 07730, México, Departamento de Química, Centro de Investigación y de Estudios Avanzados, A. P. 14-740, México, D. F., 07000, México, and Departamento de Química, División de Ciencias Básicas e Ingeniería, Universidad Autónoma Metropolitana-Iztapalapa, A. P. 55-534, México, D. F., 09340, México

Received: December 8, 2005; In Final Form: March 7, 2006

Four molecules that have been proven to act as corrosion inhibitors of mild steel in acidic media are studied. The inhibitive efficiency of these molecules is explained by means of electronic structure calculations of the protonated species that seem to represent better the actual situation of the experimental conditions. By assuming that the interaction between the inhibitor and the metallic surface occurs through donation and back-donation, it is shown, with a simple charge transfer model, that the interaction energy is favored when hardness increases, in agreement with the experimentally observed inhibition efficiencies. A local analysis with Hirshfeld condensed Fukui functions, and local Fukui functions, provides further support to the donation and back-donation mechanism.

1. Introduction

The use of corrosion inhibitors constitutes one of the most economical ways to preserve industrial facilities.[1] Molecular design has become a very useful tool for the synthesis of corrosion inhibitors that not only allows one to control the corrosion rate but at the same time also fulfills environmental protection standards. In this context, the treatment of mild steel corrosion in an acidic environment through organic compounds has resulted in considerable savings to the oil industry. In particular, it has been found that pyridine derivatives[2−6] and some 1,3-azoles[7−10] (benzoazoles and azolo[4,5-*b*]-pyridines) are among the most effective corrosion inhibitors in aggressive media. The relationship between the molecular structure of pyridine compounds as well as 1,3-azole derivatives and their inhibitive efficiency has been explored through the use of electrochemical techniques,[11−13] surface analysis,[14,15] and theoretical studies.[16−18]

On the basis of the high efficiency of these molecules, Likhanova et al.[19] performed the synthesis to integrate in a unique compound one molecule of pyridine and one molecule of 1,3-azole to study the inhibitive behavior of the synthesized compounds of 2-pyridyl-1,3-azoles and azolo[4,5-*b*]pyridines. An outstanding feature of 2-pyridyl-azoles is their biological activity;[20−22] however, their use as corrosion inhibitors has not been reported in the literature.

The synthesized compounds included 2-pyridin-2yl-1*H*-benzimidazole (**1a**), 2-pyridin-2-yl-oxazolo[4,5-*b*]pyridine (**2a**), 2-pyridin-2-yl-1*H*-imidazo[4,5-*b*]pyridine (**3a**), and 2-pyridin-2-yl-benzoxazole (**4a**) (Figure 1). After gravimetric and electrochemical measurements on mild steel, in an acidic environment (pH 3.5), it was found that the inhibition efficiency followed the order **1a** > **2a** ≥ **3a** > **4a**. It is important to note that under testing conditions the inhibitors are found in their protonated forms.

Now, the corrosion process occurs on metallic surfaces where active sites are present. That is, the metal surface has a uniform electronic density distribution, except at some specific points, where there may be an excess or deficiency of charge. These points become the active sites, where the deterioration process starts as a consequence of the attack of molecular oxygen, water, or aggressive species. To prevent that by the corrosion agent, the inhibitor must be absorbed by the metal surface over the active sites, through interactions that do not lead to a significant change in the mechanical properties of the metal surface. For the above inhibitors, the interaction with the metal surface could be understood through an electron donation process from the metal surface to the inhibitor molecule and a back-donation from the inhibitor molecule to the metal surface,[23−25] so that the charge density in the active site remains practically unchanged.

The objective of the present work is to derive a simple charge transfer model for donation and back-donation, using a density functional approach, to try to explain the inhibitive capacity of the four 2-pyridyl-1,3-azole (**1a** and **4a**) and 2-pyridyl-azolo-[4,5-*b*]pyridine (**3a** and **2a**) compounds, in terms of their different stabilization energies, when they interact with the metal surface, and to study their local selectivity, through the Fukui function, to try to understand how these molecules interact with the metal surface.

2. Simple Charge Transfer Model for Donation and Back-Donation

According to density functional theory, the chemical potential, μ, the electronegativity, χ, the hardness, η, and the softness, S, of a chemical species are given by[26−28]

$$\mu = -\chi = (\partial E/\partial N)_v, \tag{1}$$

$$\eta = (\partial^2 E/\partial N^2)_v = (\partial \mu/\partial N)_v, \quad \text{and} \quad S = 1/\eta = (\partial N/\partial \mu)_v \tag{2}$$

* Authors for correspondence. E-mail: bgomez@cinvestav.mx, jlgm@xanum.uam.mx.
† Instituto Mexicano del Petróleo.
‡ Centro de Investigación y de Estudios Avanzados.
§ Universidad Autónoma Metropolitana-Iztapalapa.

10.1021/jp057143y CCC: $33.50
Published on Web 04/19/2006

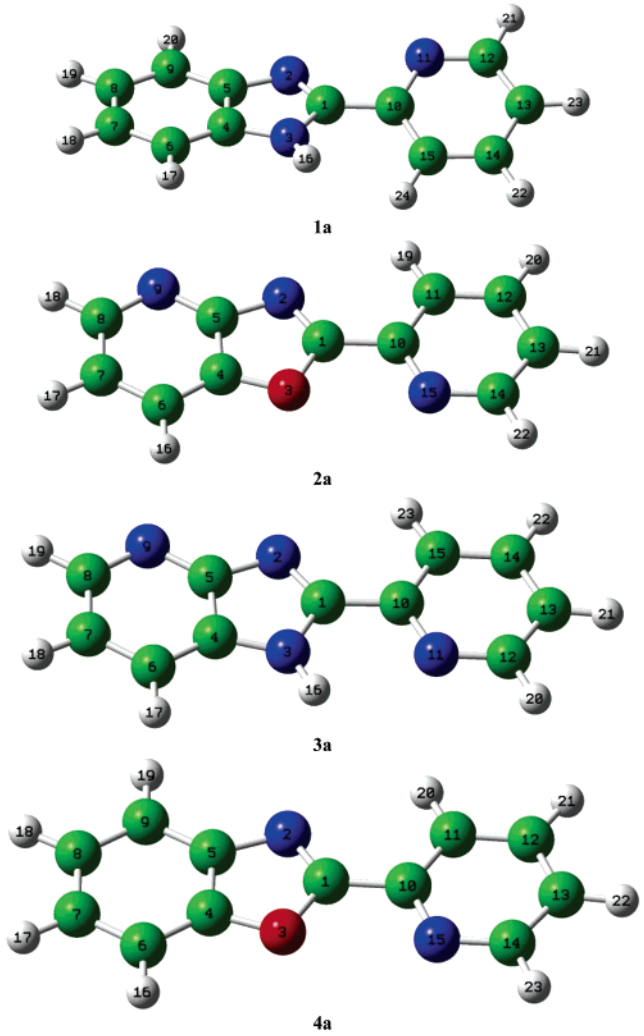

Figure 1. Unprotonated inhibitor molecules considered in the present study. Green color corresponds to carbon, blue to nitrogen, red to oxygen, and gray to hydrogen.

where E is the total electronic energy, N is the total number of electrons, and $v(\mathbf{r})$ is the external potential generated by the nuclei (the factor of $^1/_2$ in the original definition of the global hardness has been omitted here for convenience). Thus, through these definitions, it has been possible to quantify these important reactivity criteria, and through their values and the principles associated with them, it has been possible to understand the behavior of a wide variety of chemical systems, under different circumstances.

Simple charge transfer models within the framework of density functional theory are based on the Taylor series expansion of the energy as a function of the number of electrons, N, and the external potential, $v(\mathbf{r})$, which, upon neglecting all the terms associated with changes in the latter, and keeping terms up to second order in the former, leads to $\Delta E = \mu\Delta N + {}^1/_2\eta(\Delta N)^2$. This expression may be considered as a quadratic smooth interpolation between the energy values $E(N-1)$, $E(N)$, and $E(N+1)$, which implies that $\mu = -(I+A)/2$ and $\eta = I - A$ for the isolated reactant molecule. The quantities I and A denote the vertical ionization potential and electron affinity, respectively. Despite its simplicity, this expression has proven to be very useful to describe, at least qualitatively, charge transfer effects.[26−28] In particular, the electrophilicity index of Parr, Szentpály, and Liu[29] is defined through this expression to measure the second-order energy change of an electrophile as it is saturated with electrons. It is also worth mentioning that recently it has also been used by Ayers[30] and by Chattaraj and Ayers[31] to derive a simple proof of the hard and soft acids and bases principle.

However, it is important to note that, because of the nature of the energy behavior as a function of the number of electrons at zero temperature, the energy derivative of eq 1 evaluated at some integral value of N will, in general, have one value when evaluated from the left and a different value when evaluated from the right.[32] That is,

$$\mu^+ = -\chi^+ = (\partial E/\partial N)_v^+ = -A \tag{3}$$

when N increases from $N \rightarrow N+1$ and

$$\mu^- = -\chi^- = (\partial E/\partial N)_v^- = -I \tag{4}$$

when N decreases from $N \rightarrow N-1$. At zero temperature, the hardness, eq 2, is zero when the derivatives are taken from the right or the left, and it is infinite when a central difference formula is used. However, Ayers and Parr[33] have shown that some information remains, since

$$\eta(M) = (\mu^+ - \mu^-)\delta(M-N) = (I-A)\delta(M-N) \tag{5}$$

for $N-1 < M < N+1$.

Despite the mathematical difficulties associated with the derivatives of the energy with respect to the number of electrons, the discontinuities are important from the chemical viewpoint, because they predict a different response to nucleophilic and electrophilic attack. Note that the smooth quadratic interpolation approximation formula does not distinguish between these two attacks.

In this context, let us consider the situation corresponding to a molecule that is going to receive a certain amount of charge at some center and is going to back-donate a certain amount of charge through the same center, or another one. To describe the energy change associated with these two processes, we may regard the second-order simple charge transfer formula as a two-parameter expression, in which the donation and back-donation processes are differentiated through the use of different values of the chemical potential for each case, while the hardness is fixed to the value of $\eta = (\mu^+ - \mu^-)$ in both situations. Thus, for the case in which the molecule receives a certain amount of charge, ΔN^+,

$$\Delta E^+ = \mu^+\Delta N^+ + \frac{1}{2}\eta(\Delta N^+)^2 \tag{6}$$

while when the molecule back-donates a certain amount of charge, ΔN^-, then

$$\Delta E^- = \mu^-\Delta N^- + \frac{1}{2}\eta(\Delta N^-)^2 \tag{7}$$

If the total energy change is approximated by the sum of the contributions in eqs 6 and 7 and assuming that the amount of charge back-donated is equal to the amount of charge received, $\Delta N^- = -\Delta N^+$, then

$$\Delta E_T = \Delta E^+ + \Delta E^- = (\mu^+ - \mu^-)\Delta N^+ + \eta(\Delta N^+)^2 \tag{8}$$

The most favorable situation corresponds to the case when the total energy change becomes a minimum with respect to ΔN^+, which implies that $\Delta N^+ = -(\mu^+ - \mu^-)/2\eta$ and that

$$\Delta E_T = -\frac{(\mu^+ - \mu^-)^2}{4\eta} = -\frac{\eta}{4} \quad (9)$$

where we have used eq 5 for the second equality. Notice that, since $\eta > 0$, $\Delta E_T < 0$, a result that implies that the charge transfer to a molecule, followed by a back-donation from the molecule is energetically favorable. However, it is important to note that eq 9 does not predict that a back-donation process is going to occur; it only establishes that if both processes occur (charge transfer to the molecule and back-donation from the molecule), the energy change is directly proportional to the hardness of the molecule. In this context, eq 9 may be useful for a family of similar molecules, which are known to back-donate the charge they receive, because then the stabilization will increase as the hardness increases among the members of the family, given that they are interacting with the same metal surface.

3. Fukui Function and Local Selectivity

The model for back-donation derived in the previous section allows one to characterize the family of molecules from a global point of view, since the hardness does not depend on the position within the molecule. Thus, to analyze the behavior of the different sites, it is necessary to consider reactivity criteria of local type, like the Fukui function,[26] $f(\mathbf{r}) \equiv (\partial\rho(\mathbf{r})/\partial N)_v = (\delta\mu/\delta v(\mathbf{r}))_N$. As in the case for the chemical potential, the derivative of the electronic density for an N-electron system, $\rho_N(\mathbf{r})$, with respect to the total number of electrons will have one value when evaluated from the left and a different value when evaluated from the right. That is,

$$f^+(\mathbf{r}) \equiv \left(\frac{\partial\rho(\mathbf{r})}{\partial N}\right)_v^+ = \left(\frac{\delta\mu^+}{\delta v(\mathbf{r})}\right)_N = \rho_{N+1}(\mathbf{r}) - \rho_N(\mathbf{r}) \quad (10)$$

when N increases from $N \rightarrow N + 1$ and

$$f^-(\mathbf{r}) \equiv \left(\frac{\partial\rho(\mathbf{r})}{\partial N}\right)_v^- = \left(\frac{\delta\mu^-}{\delta v(\mathbf{r})}\right)_N = \rho_N(\mathbf{r}) - \rho_{N-1}(\mathbf{r}) \quad (11)$$

when N decreases from $N \rightarrow N - 1$. Thus, the molecular sites with large values of $f^+(\mathbf{r})$ are the sites where the molecule will receive charge, when attacked by a nucleophilic reagent, and the molecular sites with large values of $f^-(\mathbf{r})$ are the preferred sites through which the molecule will donate charge when attacked by an electrophilic reagent.

A useful approach to the molecular Fukui function is provided by the condensed Fukui functions.[34,35] To calculate these, one must adopt a partitioning scheme of the electronic density among the constituent atoms, to assign a net charge to each one of them. That is, if $\rho_N^i(\mathbf{r})$ is the electronic density of the ith atom in the N-electron molecule and Z_i is its nuclear charge, then the net charge of the ith atom in the molecule is given by $q_N^i = Z_i - \int\rho_N^i(\mathbf{r})\, d\mathbf{r}$, and the condensed Fukui functions may be obtained from

$$f_i^+ = \int (\partial\rho_N^i(\mathbf{r})/\partial N)_v^+ \, d\mathbf{r} = q_N^i - q_{N+1}^i \quad (12)$$

and

$$f_i^- = \int (\partial\rho_N^i(\mathbf{r})/\partial N)_v^- \, d\mathbf{r} = q_{N-1}^i - q_N^i \quad (13)$$

where q_{N+1}^i and q_{N-1}^i represent the net charge of the ith atom in the molecule with $N + 1$ and $N - 1$ electrons, respectively. Thus, for a given partitioning scheme, the calculation of the condensed Fukui functions is straightforward. In this work, we will make use of the Hirshfeld stockholders partitioning,[36−40] because it has been found that it leads to the most consistent values.[41−46] It is important to note that, recently, Roy et al.[47] have shown that these local reactivity descriptors are not always reliable in explaining intermolecular reactivity sequences. However, in the present case, these descriptors can be used because the chemical systems chosen here are of comparable size and chemical nature.

To analyze the possible sites of the molecule that will receive charge from the metal surface, one must look for the largest values of $f^+(\mathbf{r})$ or f_i^+, while to analyze the possible sites through which the molecule will back-donate charge to the metal surface, one must look for the largest values of $f^-(\mathbf{r})$ or f_i^-.

4. Computational Details

The electronic structure of the four molecules considered in this work was determined through the density functional deMon2k computational package.[48] The molecular structures and the Fukui functions were visualized using GaussView[49] and VU,[50] respectively. All calculations were carried out using the BLYP exchange and correlation energy functionals,[51,52] with a TZVP[53,54] orbital basis set in combination with a GEN-A2* auxiliary basis set. Full geometry optimizations were performed for all of the cases considered, followed up by frequency calculations to characterize the stationary points obtained in the geometry optimization.

Since, under testing conditions, the prototype inhibitors are protonated, we have carried out a complete study of all single protonated structures in all of the possible sites (heteroatom positions), because, at the experimental pH of 3.5, one should not expect multiple protonation to occur. Thus, the proton affinity, PA, was calculated for all of the combinations, and the most stable structure was selected for each of the four inhibitors, to perform the reactivity analysis on the selected protonated molecules.

The hardness and the Fukui functions were determined through finite differences by performing, at the geometry of the reference protonated N-electron inhibitor, the calculations for the $N + 1$ and $N - 1$ electron species.

5. Results and Discussion

The optimized geometries of the four molecules, before protonation, are presented in Figure 1. It may be observed that molecule **1a** shows a nonplanar geometry, while the other three molecules show an almost planar geometry. The dihedral angle N2−C1−C10−C11 is 24.3, 0.8, and 0.6° for the molecules **1a**, **2a**, and **4a**, respectively, while the dihedral angle N2−C1−C10−C15 for molecule **3a** is 0.0°.

The results for the optimized geometries of the protonated species are presented in Figures 2−5, and the values of the proton affinities are reported in Table 1. It is important to mention that although all of the possible protonation sites for the four inhibitors were considered, it was found that, in the case of the **2a** and **4a** molecules, the proton on the oxygen atom migrated to the nitrogen atom of pyridine during the geometry optimization process.

It can be observed in Figures 2−5 that, in contrast with the unprotonated ground state species, the protonated ones show a high degree of planarity, that may lead to a high electronic delocalization, typical of a resonant system. This situation indicates that the molecular interaction with the metallic surface possibly occurs through the π orbitals of the imidazolinic or pyramidinic rings.

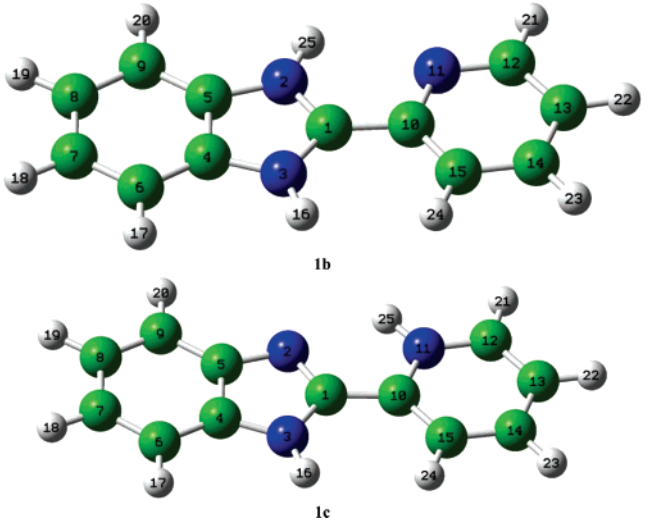

Figure 2. Protonated forms for the molecule **1a**, see Figure 1.

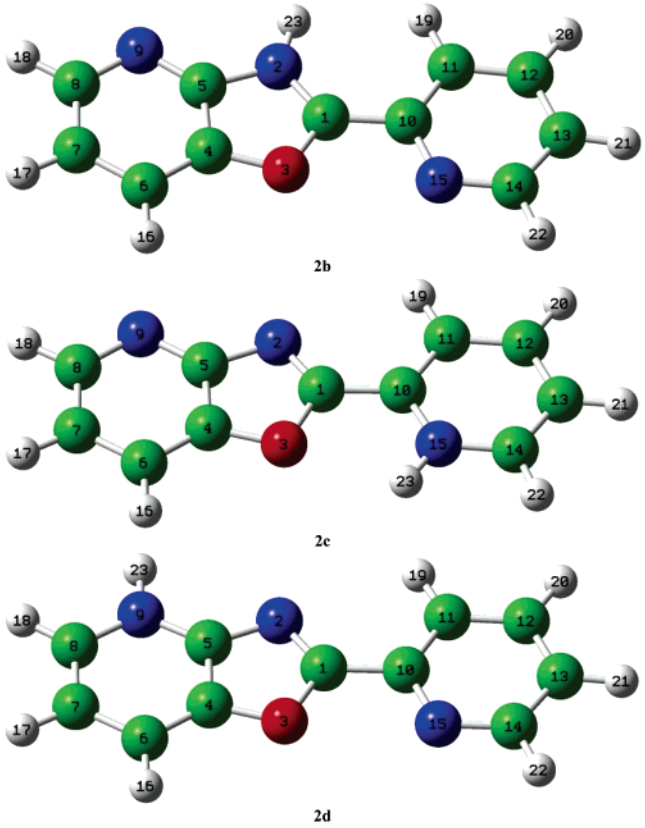

Figure 3. Protonated forms for the molecule **2a**, see Figure 1.

In relation with the protonation sites for the four species considered in this work, it was found that, for molecule **1a**, by a difference of 3.84 kcal/mol (Table 1), the most stable form corresponds to the case when the proton binds at the nitrogen N-2 of imidazoline, molecule **1b** (Figure 2). Three protonated species were found for molecule **2a** (Figure 3), and the one protonated on nitrogen N-9, molecule **2d**, was found to be more stable than the ones on atoms N-2 and N-15, by a difference of 8.47 and 3.47 kcal/mol, respectively. For inhibitor **3a**, the protonated structure on N-9, molecule **3c**, is more stable than the other two homologous structures with the proton on atoms N-2 and N-11 (Figure 4), by a difference of 4.48 and 10.15 kcal/mol, respectively. In the case of molecule **4a**, there are two likely forms (Figure 5) that may be present when one of the nitrogen atoms is protonated; the most stable form was found

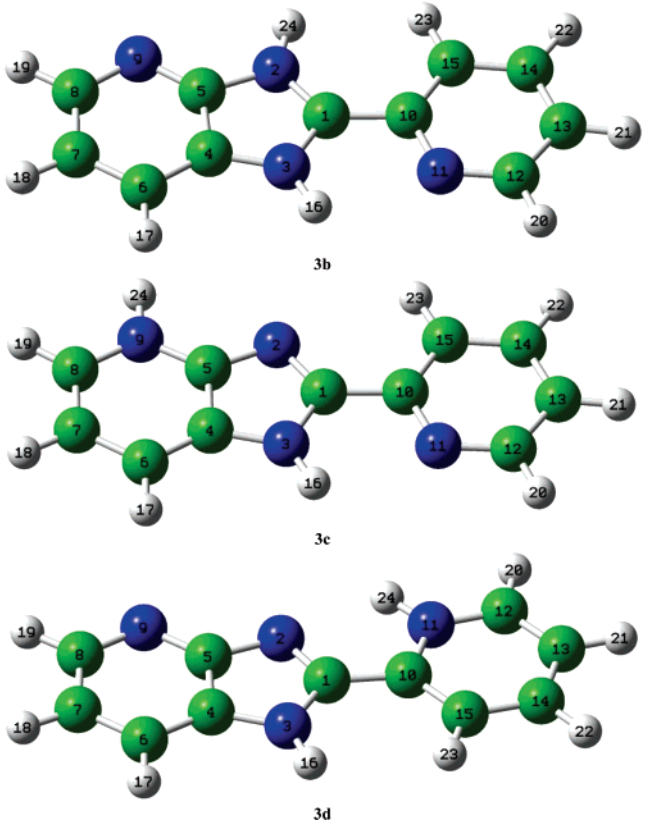

Figure 4. Protonated forms for the molecule **3a**, see Figure 1.

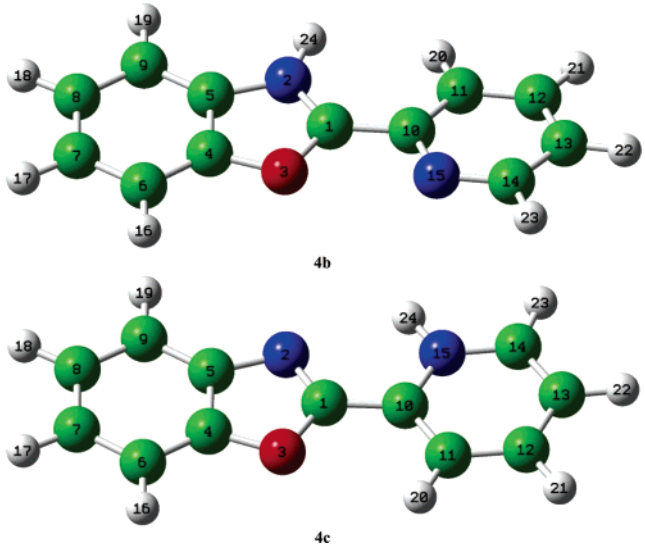

Figure 5. Protonated forms for the molecule **4a**, see Figure 1.

TABLE 1: Proton Affinities, in kcal/mol, of the Protonated Forms Considered for the Four Inhibitors

molecule	PA	molecule	PA
1b	248.94	**3b**	238.73
1c	245.16	**3c**	243.52
2b	226.72	**3d**	233.07
2c	232.16	**4b**	228.19
2d	235.69	**4c**	235.96

for the case when the proton binds to N-15, molecule **4c**, by a difference of 7.27 kcal/mol.

The rotation barriers of the pyridine ring around carbon atoms C-1 and C-10 were analyzed for the four inhibitors in their most stable protonated forms, and the results are presented in Figure 6. The energy barriers are 8.05, 8.31, 12.60, and 3.43 kcal/mol

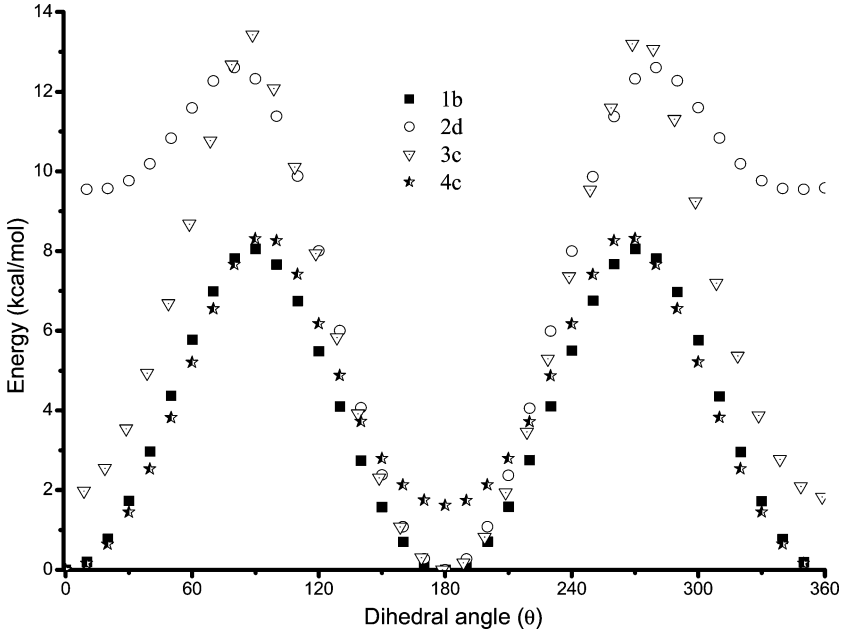

Figure 6. Rotational energy barrier for the most stable protonated form of the four molecules.

TABLE 2: Chemical Hardness, in eV, of the Unprotonated Molecules and of the More Stable Protonated Forms

unprotonated molecules	η	protonated molecules	η
1a	7.29	**1b**	7.21
2a	7.39	**2d**	6.96
3a	7.17	**3c**	6.91
4a	7.43	**4c**	6.30

TABLE 3: Condensed Fukui Functions for the Case When the Molecule Receives Charge from the Metal Surface

	molecules							
	1b		**2d**		**3c**		**4c**	
number	atom	f_i^+	atom	f_i^+	atom	f_i^+	atom	f_i^+
1	C	0.075	C	0.074	C	0.068	C	0.026
2	N	0.047	N	0.044	N	0.042	N	0.060
3	N	0.046	O	0.034	N	0.027	O	0.030
4	C	0.018	C	0.029	C	0.029	C	0.025
5	C	0.017	C	0.046	C	0.041	C	0.021
6	C	0.044	C	0.095	C	0.095	C	0.030
7	C	0.051	C	0.055	C	0.053	C	0.053
8	C	0.049	C	0.076	C	0.080	C	0.038
9	C	0.043	N	0.062	N	0.061	C	0.035
10	C	0.043	C	0.017	C	0.019	C	0.072
11	N	0.050	C	0.039	N	0.032	C	0.042
12	C	0.045	C	0.037	C	0.035	C	0.092
13	C	0.080	C	0.063	C	0.062	C	0.067
14	C	0.051	C	0.036	C	0.039	C	0.065
15	C	0.049	N	0.035	C	0.037	N	0.062
16	H	0.026	H	0.044	H	0.022	H	0.021
17	H	0.026	H	0.035	H	0.044	H	0.029
18	H	0.030	H	0.041	H	0.034	H	0.026
19	H	0.029	H	0.019	H	0.042	H	0.022
20	H	0.025	H	0.026	H	0.024	H	0.028
21	H	0.030	H	0.033	H	0.032	H	0.046
22	H	0.041	H	0.025	H	0.026	H	0.039
23	H	0.032	H	0.037	H	0.019	H	0.037
24	H	0.027			H	0.037	H	0.034
25	H	0.027						

for **1b**, **2d**, **3c**, and **4c**, respectively. These small barriers seem to indicate that rotational effects, at room temperature, will not constitute a differentiation factor for the corrosion inhibition capacity.

Now, if it is assumed that the inhibitor efficiency should increase when there is a better adsorption of the molecule to the metal surface, then the inhibition efficiency should increase when the stabilization energy that results from the interaction between the metal surface and the inhibitor increases. Thus, taking into account that the interaction of this type of molecules with metal surfaces occurs, in general, through donation and back-donation, then, according to eq 9, the stabilization energy increases when the hardness increases, within a family of molecules. In Table 2, we present the hardness values calculated for the ground state of the four protonated molecules with eq 5. It may be noted that the hardness of the protonated molecules follows the order **1b** > **2d** = **3c** > **4c**, which is in agreement with the efficiency experimentally calculated by potentiodynamic polarization for these inhibitors. This result seems to suggest that, due to the planar geometry of the four protonated

TABLE 4: Condensed Fukui Functions for the Case When the Molecule Back-Donates Charge to the Metal Surface

	molecules							
	1b		**2d**		**3c**		**4c**	
number	atom	f_i^-	atom	f_i^-	atom	f_i^-	atom	f_i^-
1	C	0.036	C	0.000	C	0.026	C	0.067
2	N	0.028	N	0.056	N	0.052	N	0.048
3	N	0.025	O	0.013	N	0.026	O	0.033
4	C	0.053	C	0.014	C	0.042	C	0.035
5	C	0.057	C	0.014	C	0.029	C	0.069
6	C	0.037	C	0.027	C	0.042	C	0.066
7	C	0.082	C	0.037	C	0.060	C	0.105
8	C	0.075	C	0.041	C	0.069	C	0.052
9	C	0.037	N	0.020	N	0.027	C	0.062
10	C	0.038	C	0.050	C	0.059	C	0.012
11	N	0.027	C	0.051	N	0.033	C	0.040
12	C	0.055	C	0.062	C	0.074	C	0.036
13	C	0.078	C	0.054	C	0.090	C	0.057
14	C	0.039	C	0.068	C	0.043	C	0.043
15	C	0.049	N	0.221	C	0.064	N	0.021
16	H	0.021	H	0.016	H	0.020	H	0.035
17	H	0.028	H	0.021	H	0.026	H	0.043
18	H	0.037	H	0.022	H	0.031	H	0.034
19	H	0.036	H	0.045	H	0.031	H	0.034
20	H	0.028	H	0.048	H	0.036	H	0.017
21	H	0.029	H	0.045	H	0.039	H	0.023
22	H	0.034	H	0.059	H	0.031	H	0.028
23	H	0.027	H	0.014	H	0.029	H	0.024
24	H	0.023			H	0.021	H	0.014
25	H	0.021						

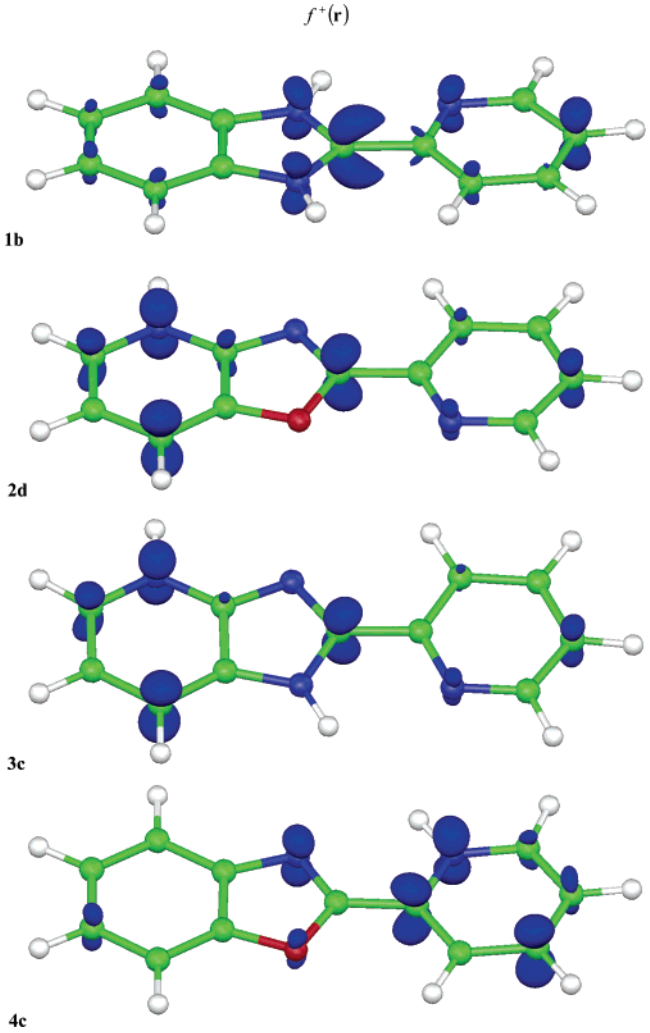

Figure 7. Isosurfaces of the local Fukui functions $f^+(\mathbf{r})$ for the most stable protonated form of the four molecules. The isosurface value is 0.007 au for all cases; see Figure 1.

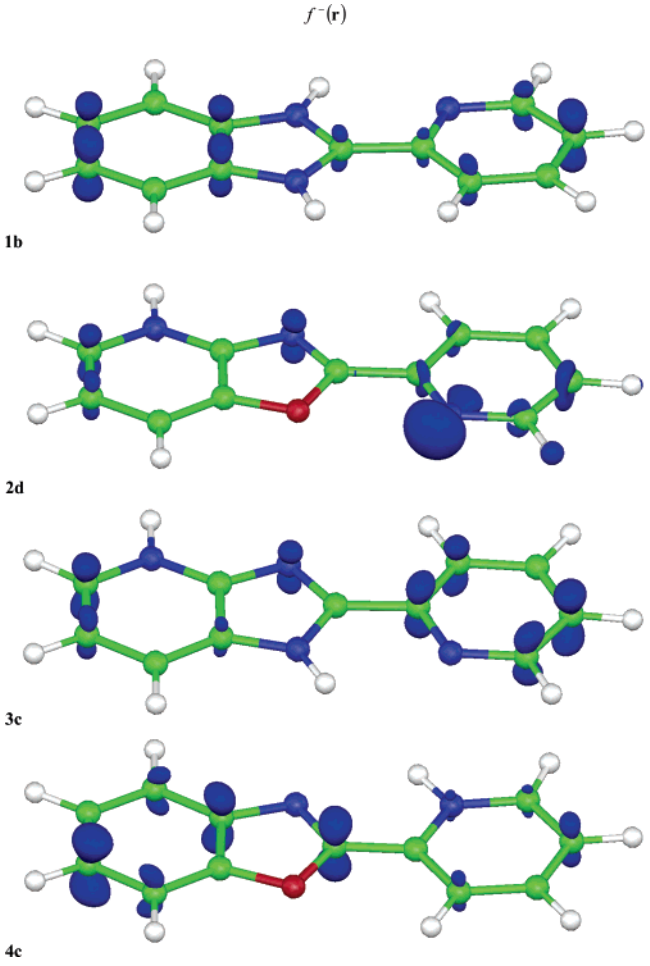

Figure 8. Isosurfaces of the local Fukui function $f^-(\mathbf{r})$ for the most stable protonated form of the four molecules. The isosurface value is 0.007 au for all cases; see Figure 1.

species (the dihedral angle reported for the unprotonated species is 0.0° for the protonated molecules **1b**, **2d**, **3c**, and **4c**), the molecular adsorption probably occurs in such a way that the metal surface and the molecular plane are parallel to each other, and that, in this conformation, the interaction is dominated by donation and back-donation between the molecule and the metallic surface. It is important to note that the hardness of the unprotonated species follows a different order from the inhibition efficiency experimentally obtained. Such result could support the assumption that, in acidic media, the most stable protonated forms are responsible for the interaction with the metal surface. Additionally, it can also be observed in Table 2 that the protonated species are softer than their unprotonated counterparts. Since the softer a molecule, the more reactive it becomes, this result also seems to favor the protonated species for the interaction with the metal surface in acidic media.

The analysis of the local behavior may be carried out through the Fukui functions $f^+(\mathbf{r})$ or f_i^+, when the inhibitor molecule receives charge from the metal, and through $f^-(\mathbf{r})$ or f_i^-, when the inhibitor molecule donates charge to the metal. The results for the condensed Fukui functions, f_i^+ and f_i^-, are presented in Tables 3 and 4, while the results for the Fukui functions, $f^+(\mathbf{r})$ and $f^-(\mathbf{r})$, are presented in Figures 7 and 8. It may be observed that the condensed and local Fukui functions, f_i^+ and $f^+(\mathbf{r})$, respectively, have large values at the carbon atoms C-1 and C-13 in the case of the best inhibitor molecule, **1b**, and that the values at these two carbon atoms decrease following the same order of the inhibitive efficiency in the case of the other three molecules. By recalling that the four protonated molecules have a net positive charge, one could assume that the interaction with the metal surface will probably occur at sites where this one has an excess of charge that will be donated to the inhibitor molecule. Thus, although the Fukui function has also considerable values at other atoms, one could conclude that, for the molecules **1b**, **2d**, and **3c**, the carbon atoms C-1 and C-13 will play a significant role in the interaction with the metal surface, while, for the worst inhibitor molecule, **4c**, the interaction will probably occur through other atoms.

Now, for the back-donation from the molecule to the metal surface, one must consider f_i^- and $f^-(\mathbf{r})$. In this case, one can observe that the condensed and local Fukui functions at C-1 are practically equal to zero, for molecules **1b**, **2d**, and **3c**, while, for the worst inhibitor, **4c**, C-1 has a large value. It can also be observed that the molecule **1b** has large values at C-4, C-5, C-7, and C-8 of the imidazolinic ring, molecules **2d** at C-10, C-11, C-13, and C-14 of the pyramidinic ring, and **3c** at C-10, C-12, C-13, and C-15 also of the pyramidinic ring. In the three cases, the four carbon atoms encompass a large contribution to the π orbital, which is probably responsible for the back-donation. It is important to note that the relatively large values of C-13 in the case of molecules **2d** and **3c** are due to the fact that in these two cases it forms part of the π orbital, which is basically located at the pyramidinic ring. On the other hand, for the worst inhibitor, **4c**, the large values appear to be more

dispersed through the entire molecule, maybe indicating a less effective donation and back-donation mechanism.

6. Concluding Remarks

Although the present approach needs to be applied to other families of planar compounds that have been tested as corrosion inhibitors for mild steel in an acidic environment, the results presented in this work indicate that, indeed, in acidic media, one should consider the protonated structures of the species involved because they seem to represent better the actual experimental situation. Additionally, back-donation appears to be the underlying electronic mechanism driving the interaction between the inhibitor molecule and the metal surface. A simple charge transfer model for back-donation and a local and condensed Fukui function analysis of the reactive sites of the molecules have been shown to be very useful in rationalizing the inhibitive efficiency of pyridyl-azole type molecules.

Acknowledgment. B.G., N.V.L., and R.M.-P. thank CONACyT for the complementary grant provided. A.V. appreciates partial support from CONACyT grant 47175-F.

References and Notes

(1) Sastri, V. S. *Corrosion Inhibitors. Principles and Applications*; John Wiley & Sons: New York, 1998.
(2) Chatterjee, P.; Singh, D. D. N. *Anti-Corros. Methods Mater.* **1991**, *38*, 4−10.
(3) Kliskic, M.; Radosevic, J.; Gudic, S. *J. Appl. Electrochem.* **1997**, *27*, 947−952.
(4) Bouklah, M.; Attayibat, A.; Hammouti, B.; Ramdani, A.; Radi, S.; Benkaddour, M. *Appl. Surf. Sci.* **2005**, *240*, 341−348.
(5) El-Maksouda, S. A. A.; Fouda, A. S. *Mater. Chem. Phys.* **2005**, *93*, 84−90.
(6) Tebbji, K.; Oudda, H.; Hammouti, B.; Benkaddour, M.; El Kodadi, M.; Ramdani, A. *Colloids Surf., A* **2005**, *259*, 143−149.
(7) Muralidharan, S.; Iyer, S. V. *Anti-Corros. Methods Mater.* **1997**, *44*, 100−106.
(8) Popova, A.; Christov, M.; Deligeorgiev, T. *Corrosion* **2003**, *59*, 756−764.
(9) Bereket, G.; Pinarbasi, A.; Ogretir, C. *Anti-Corros. Methods Mater.* **2004**, *51*, 282−293.
(10) Morales-Gil, P.; Negron-Silva, G.; Romero-Romo, M.; Angeles-Chavez, C.; Palomar-Pardave, M. *Electrochim. Acta* **2004**, *49*, 4733−4741.
(11) Popova, A.; Raicheva, S.; Sokolova, E.; Christov, M. *Langmuir* **1996**, *12*, 2083−2089.
(12) Al-Mayouf, A. M.; Al-Suhybani, A. A.; Al-Ameery, A. K. *Desalination* **1998**, *116*, 25−33.
(13) Yurt, A.; Balaban, A.; Kandemir, S. U.; Bereket, G.; Erk, B. *Mater. Chem. Phys.* **2004**, *85*, 420−426.
(14) Fleischmann, M.; Hill, I. R.; Mengoli, G.; Musiani, M. M.; Akhavan, J. *Electrochim. Acta* **1985**, *30*, 879−888.
(15) El Azhar, M.; Traisnel, M.; Mernari, B.; Gengembre, L.; Bentiss, F.; Lagrenee, M. *Appl. Surf. Sci.* **2002**, *185*, 197−205.
(16) Bentiss, F.; Lebrini, M.; Vezin, H.; Lagrenee, M. *Mater. Chem. Phys.* **2004**, *87*, 18−23.
(17) Xiao-Ci, Y.; Hong, Z.; Ming-Dao, L.; Hong-Xuan, R.; Lu-An, Y. *Corros. Sci.* **2000**, *42*, 645−653.
(18) Vosta, J.; Eliasek, J. *Corros. Sci.* **1971**, *11*, 223−229.
(19) Likhanova, N. V.; Veloz, M. A.; Hopfl, H.; Matias, D. J.; Garibay-Febles, V.; Reyes-Cruz, V. E.; Martínez-Palou, R. Submitted to *J. Het. Chem.*
(20) Weier, R. M.; Khanna, I. K.; Stealy, M. A.; Julien, J. A. U.S. Patent 5,262,426, 1993.
(21) Shen, T. Y.; Clark, R. L.; Pessolano, A. A.; Witzel, B. E.; Lanza, T. J. U.S. Patent 4,038,396, 1977.
(22) Abitz, W.; Morf, D. F.; Brauns, H. A. DE Patent 2,330,109, 1973.
(23) Aramaki, K. *Corros. Eng.* **1983**, *32*, 253−257.
(24) Chakrabarti, A. *Br. Corros. J.* **1984**, *19*, 124−126.
(25) Crabtree, R. H. *The Organometallic Chemistry of the Transition Metals*, 3rd ed.; John Wiley & Sons: New York, 2001.
(26) Parr, R. G.; Yang, W. *Density-Functional Theory of Atoms and Molecules*; Oxford University Press: New York, 1989.
(27) Geerlings, P.; De Proft, F.; Langenaeker, W. *Chem. Rev.* **2003**, *103*, 1793−1873.
(28) Chermette, H. *J. Comput. Chem.* **1999**, *20*, 129−154.
(29) Parr, R. G.; Von Szentpaly, L.; Liu, S. B. *J. Am. Chem. Soc.* **1999**, *121*, 1922−1924.
(30) Ayers, P. W. *J. Chem. Phys.* **2005**, *122*.
(31) Chattaraj, P. K.; Ayers, P. W. *J. Chem. Phys.* **2005**, *123*.
(32) Perdew, J. P.; Parr, R. G.; Levy, M.; Balduz, J. L. *Phys. Rev. Lett.* **1982**, *49*, 1691−1694.
(33) Ayers, P. W.; Parr, R. G. *J. Am. Chem. Soc.* **2000**, *122*, 2010−2018.
(34) Yang, W.; Mortier, W. J. *J. Am. Chem. Soc.* **1986**, *108*, 5708−5711.
(35) Ayers, P. W.; Morrison, R. C.; Roy, R. K. *J. Chem. Phys.* **2002**, *116*, 8731−8744.
(36) Hirshfeld, F. L. *Theor. Chim. Acta* **1977**, *44*, 129−138.
(37) Nalewajski, R. F.; Parr, R. G. *Proc. Natl. Acad. Sci. U.S.A.* **2000**, *97*, 8879−8882.
(38) Nalewajski, R. F.; Parr, R. G. *J. Phys. Chem. A* **2001**, *105*, 7391−7400.
(39) Nalewajski, R. F. *Phys. Chem. Chem. Phys.* **2002**, *4*, 1710−1721.
(40) Nalewajski, R. F. *Adv. Quantum Chem.* **2003**, *43*, 119−184.
(41) Roy, R. K.; Pal, S.; Hirao, K. *J. Chem. Phys.* **1999**, *110*, 8236−8245.
(42) Roy, R. K.; Hirao, K.; Pal, S. *J. Chem. Phys.* **2000**, *113*, 1372−1379.
(43) Roy, R. K. *J. Phys. Chem. A* **2003**, *107*, 10428−10434.
(44) Roy, R. K. *J. Phys. Chem. A* **2004**, *108*, 4934−4939.
(45) De Proft, F.; Van Alsenoy, C.; Peeters, A.; Langenaeker, W.; Geerlings, P. *J. Comput. Chem.* **2002**, *23*, 1198−1209.
(46) De Proft, F.; Vivas-Reyes, R.; Peeters, A.; Van Alsenoy, C.; Geerlings, P. *J. Comput. Chem.* **2003**, *24*, 463−469.
(47) Roy, R. K.; Usha, V.; Paulovic, J.; Hirao, K. *J. Phys. Chem. A* **2005**, *109*, 4601−4606.
(48) Koster, A. M.; Calaminici, P.; Casida, M. E.; Flores-Moreno, R.; Geudtner, G.; Goursot, A.; Heine, T.; Ipatov, A.; Janetzko, F.; Patchkovskii, S.; Reveles, J. U.; Vela, A.; Salahub, D. R. *deMon2k*, version 2.0; 2005.
(49) *GaussView*, version 3.0; Gaussian, Inc.: Pittsburgh, PA, 2003.
(50) Ozell, B.; Camarero, R.; Garon, A.; Guibault, F. *Finite Elem. Des.* **1995**, *19*, 295−307.
(51) Becke, A. D. *J. Chem. Phys.* **1993**, *98*, 5648−5652.
(52) Lee, C. T.; Yang, W. T.; Parr, R. G. *Phys. Rev. B* **1988**, *37*, 785−789.
(53) Schafer, A.; Horn, H.; Ahlrichs, R. *J. Chem. Phys.* **1992**, *97*, 2571−2577.
(54) Schafer, A.; Huber, C.; Ahlrichs, R. *J. Chem. Phys.* **1994**, *100*, 5829−5835.